Published in final edited form as:
Biochemistry. 2013 October 8; 52(40): . doi:10.1021/bi400862q.

STABILITY AND STOICHIOMETRY OF BILAYER PHOSPHOLIPID-CHOLESTEROL COMPLEXES: RELATIONSHIP TO CELLULAR STEROL DISTRIBUTION AND HOMEOSTASIS[&]

Yvonne Lange[#,*], **S. M. Ali Tabei**[@], **Jin Ye**[#], and **Theodore L. Steck**[¶]

[#]Department of Pathology, Rush University Medical Center, Chicago, Illinois 60612, USA

[@]James Franck Institute, University of Chicago, Chicago, Illinois 60637, USA

[¶]Department of Biochemistry and Molecular Biology, University of Chicago, Chicago, Illinois 60637, USA

Abstract

Does cholesterol distribute among intracellular compartments by passive equilibration down its chemical gradient? If so, its distribution should reflect the relative cholesterol affinity of the constituent membrane phospholipids as well as their ability to form stoichiometric cholesterol complexes. We tested this hypothesis by analyzing the reactivity to cholesterol oxidase of large unilamellar vesicles (LUVs) containing biological phospholipids plus varied cholesterol. The rates of cholesterol oxidation differed among the various phospholipid environments by roughly four orders of magnitude. Furthermore, accessibility to the enzyme increased by orders of magnitude at cholesterol thresholds that suggested stoichiometries of association of 1:1, 2:3 or 1:2 cholesterol:phospholipid (mol:mol). Cholesterol accessibility above the threshold was still constrained by its particular phospholipid environment. One phospholipid, 1-stearoyl-2-oleoyl-sn-glycero-3-phosphatidylserine, exhibited no threshold. The analysis suggested values for the relative stabilities of the cholesterol-phospholipid complexes and for the fractions of bilayer cholesterol not in complexes at the threshold equivalence points; predictably, the saturated phosphorylcholine species had the lowest stoichiometries and the strongest affinities for cholesterol. These results were in general agreement with the equilibrium distribution of cholesterol between the various LUVs and methyl-β-cyclodextrin. In addition, the properties of the cholesterol in intact human red blood cells matched predictions made from LUVs of the corresponding composition. These results support a passive mechanism for the intracellular distribution of cholesterol that can provide a signal for its homeostatic regulation.

Sterols and phospholipids are nonuniformly distributed among the organelles of eukaryotic cells (1, 2). Cholesterol is most enriched in the plasma membrane where it serves to condense and order the polar lipids, thereby thickening, stiffening and strengthening the bilayer and reducing its passive permeability to small molecules even while increasing its fluidity (3–7). The lipids in the membranes along endocytic pathways resemble those of the plasma membrane because they share its bilayer constituents through vesicular traffic to-and-fro. The intracellular membranes, and the ER in particular, are demonstrably sterol-poor (1, 8, 9). Cholesterol circulates within the cell on a time scale of several minutes, presumably mediated by a combination of simple diffusion, collisional transfers and carrier proteins (10–13). The means by which cholesterol is apportioned to the organelles is not

[&]This work was supported by National Institutes of Health grant HL28448 to Y.L.

[*]To whom correspondence should be addressed at Department of Pathology, Rush University Medical Center, 1653 W. Congress Pkwy., Chicago, IL 60612. Tel: 312-942-5256. Fax: 312-563-3115. ylange@rush.edu.

known. It could be distributed by passive equilibration down its chemical potential gradient or by energized, targeted transport (13–15). The localization of cell cholesterol would then depend upon its affinity for the diverse organelle phospholipids. These affinities are a function of the length of the phospholipid apolar chains, their degree of unsaturation and, to a lesser extent, the makeup of the polar head groups (4, 16–24). There is also evidence that phospholipids can associate with sterols to form complexes with characteristic stoichiometries (20, 25–27). Such complexes might additionally associate into higher oligomers of varied size (26, 27) and be the basis for the formation of micro-domains or rafts (20, 28).

The apparent stoichiometries of the putative sterol:phospholipid complexes are on the order of ~1:1 to 1:3; *i.e.,* CMFs of 0.25–0.50. Cholesterol in excess of this complexing capacity would remain dissolved in the bilayer with a weaker phospholipid affinity; *i.e.,* a higher chemical activity, leaving tendency and/or reactivity which we refer to simply as its *activity* (10, 16, 26, 29). The consequent increased projection of the super-threshold sterol into the aqueous compartment would enhance its accessibility to soluble ligands and probes (13, 16, 30, 31). This heightened exposure presumably underlies the sharp rise in the rate of exit of membrane sterols when their level exceeds a threshold taken to be stoichiometric equivalence with the phospholipids (29, 32–34). Also consistent with this premise is the observation that the binding of the bacterial toxin, perfringolysin O, to membranes increases dramatically when their cholesterol content exceeds a sharp threshold (35–37).

Cells rigorously maintain their overall cholesterol levels through diverse feedback pathways. Super-threshold cholesterol in the ER and mitochondria could be the signal that elicits homeostatic responses through associations with regulatory proteins therein (13, 16, 29). However, our knowledge of the phospholipid content, composition, cholesterol affinity and binding stoichiometry of the organelle bilayers is not sufficient to establish whether the intracellular distribution and homeostasis of cholesterol is governed by the passive thermodynamic mechanism mentioned above. Furthermore, most of the support for the concept of sterol-phospholipid complexes comes from experiments based on monolayer films at low temperature and surface pressure; hence, uncertain applicability to biological systems.

We have therefore examined the behavior of the bilayer cholesterol in LUVs made from several relevant phospholipids. In one approach, we inferred the relative affinity of phospholipids for the sterol from its equilibrium distribution between LUVs and MBCD. In addition, we used cholesterol oxidase to probe cholesterol-containing LUVs because its activity is highly sensitive to the molecular environment of its substrate; see Discussion and ref. (38–41). In particular, it appears that the manner in which cholesterol associates with bilayer phospholipids limits its availability to this enzyme (16, 42–47). The enzyme would appear to act preferentially on sterol molecules not complexed with membrane phospholipids (32). Supporting this supposition are observations that a variety of membrane-intercalating amphipaths stimulate cholesterol oxidase activity, apparently by displacing the sterol from its association with phospholipids (48–50).

This study addressed the following questions: a) Does cholesterol form complexes with all types of bilayer phospholipids? b) What are the stoichiometries and the relative stabilities of these complexes? c) Does the accessibility of the cholesterol at the surface of bilayers increase when the cholesterol exceeds the putative complexing capacity of the phospholipids? d) Do the stoichiometries and affinities of the complexes account for a passive distribution of cholesterol in cells? e) Could cholesterol in excess of the capacity of the phospholipids serve as a homeostatic feedback signal?

EXPERIMENTAL PROCEDURES

Materials

Cholesterol was obtained from Steraloids, phospholipids from Avanti Polar Lipids and [4-^{14}C]cholesterol from Perkin Elmer. HPCD (ave. MW = 1396), MBCD (ave. MW = 1310) and Taloxapol (Triton WR-1339) were purchased from Sigma-Aldrich. The Amplex Red Cholesterol Assay kit was from Life Technologies. Cholesterol oxidase (EC 1.1.3.6; *Streptomyces* sp; reported activity of 43.9 U/mg protein) was obtained from EMD; it was dissolved in PBS (pH 6.6) and stored frozen in aliquots which were thawed once before use. The BCA protein assay kit was from Pierce. Avanti Polar Lipids supplied the Mini-Extruder plus holder/heating block as well as the Nuclepore extrusion filter membranes (0.2 micron, Whatman #800281) and 10 mm filter supports #610014. Centrifugal filters (Amicon Ultracel, 0.5 ml, 100 K) were used without prior washing.

LUV preparations

Organic solutions of phospholipids and cholesterol were mixed, dried under N_2, dissolved in ethanol at 37 °C, suspended in HBS to 1.0–1.6 mM total lipid by vigorous vortex mixing at 37 °C, incubated for 30 min at a temperature ≥10 °C above the melting temperature of each phospholipid and passed 13 times through a pair of unwashed Millipore 100 nm pore filters in an Avanti LUV extruder kept on a heating block at the corresponding temperature (51). Large particulates were cleared by centrifugation.

RBC preparation

Human blood was fresh, stored on ice and aliquots of erythrocytes washed in HBS (52). We determined that 1 μl of packed cells contained ~1.0×10^7 cells with ~2.5 nmol of cholesterol and ~3.1 nmol of phospholipid P. To increment their cholesterol content, red cells were incubated at 37 °C for 30 min with 5% (w/v, ~43 mM) HPCD carrying various amounts of cholesterol (typically, 0.003 to 0.01 mol/mol), then washed. The HPCD-cholesterol complexes were kept at or above room temperature to avoid cholesterol precipitation.

General analytical procedures

Cholesterol was determined with a cholesterol oxidase-Amplex Red assay kit or by HPLC (53). Phospholipid P was determined by phosphomolybdate colorimetry on organic extracts (54). Protein was analyzed in duplicate using the BCA method and a BSA standard.

Cholesterol oxidase kinetics

The effect of the cholesterol content of membranes on the activity of cholesterol oxidase was assayed in 100 μl PBS (pH 6.6) at 37 °C in microtiter wells. Mixtures contained 36 μM Amplex Red, 1.2 U. horseradish peroxidase, cholesterol oxidase and LUVs bearing ~1–6 nmol phospholipid plus varied proportions of cholesterol. Because the reactions proceeded at widely-different specific rates, the cholesterol oxidase was varied between 0.0002 and 2 IU to achieve half-times in the range of 5–60 min. The fluorescent product was measured at intervals in a Victor 3 spectrophotofluorimeter. We assume that cholesterol flip-flop was fast on this time scale and therefore not rate-determining (55). First-order oxidation of cholesterol went to completion in a few of the systems, indicating that the LUVs were unilamellar. We verified that enzyme rates varied linearly with the concentration of the enzyme as well as with phospholipid in a given experiment and were not limited by the Amplex Red cocktail. Relative accessibilities of cholesterol (RA, expressed in arbitrary units) were calculated from reaction rates according to eq. (6) in Appendix 1.

The cholesterol oxidase reaction for intact erythrocytes variously enriched in cholesterol was performed as described for the LUVs, except for the following: Reactions were performed with 0.2 IU cholesterol oxidase for 10 min at 37° C on 12.5–25 Tl packed cells (~30–60 nmol phospholipid P) in final volumes of 100 μl PBS (pH 6.6) in microfuge tubes. Reactions were stopped with 1 ml isopropanol which precipitated the proteins and extracted the lipids for HPLC analysis of residual cholesterol and the reaction product, cholest-4-en-3-one. From the release of hemoglobin to supernatants in control experiments (measured by its optical absorbance at 415 nm), we showed that hemolysis was <5 %.

Equilibrium distribution of cholesterol between LUV and MBCD

We adapted this procedure to estimate the relative cholesterol affinity of the phospholipids (19). In various experiments, reaction mixtures contained 10 mM MBCD bearing 0.02 to 0.8 mM [^{14}C]cholesterol. LUV phospholipid was varied between 0.1–0.8 mM. We included 0.3% Triton WR-1339 to reduce the adsorption of [^{14}C]cholesterol-MBCD to the filters; the agent did not disrupt the LUV or alter the partition of cholesterol. Equilibrations were performed in HBS at 25 °C or 37 °C for 0.5 h. Separation of the equilibrium mixtures was by performed by centrifugal filtration at the incubation temperature for 10 min at 12,000 × g (25 °C) or at 14,000 × g (37 °C). The distribution of the sterol was calculated from the radioactivity in the filtrate and input mixtures. Based upon controls lacking LUV, we corrected for a fairly constant ~10% loss of MBCD-[^{14}C]cholesterol to the filter; based upon controls lacking MBCD, we corrected for a fairly constant ~2% escape of LUV [^{14}C]cholesterol into the filtrate. (We assumed that binding of MBCD-[^{14}C]cholesterol to the LUV was negligible.) In a few cases, we verified the radioisotope distribution method by directly determining the cholesterol/phospholipid mass ratio in the retained LUV fraction.

The distribution of [^{14}C]cholesterol between MBCD and erythrocytes was determined using the method described above with the following exceptions. The MBCD (10 mM) was labeled with a trace of [^{14}C]cholesterol and incubated at 37 °C for one hour with erythrocytes (~100–400 μl cells containing ~0.3–1.2 μmoles phospholipid P) enriched to contain ~0.25–1.0 μmoles of cholesterol. After centrifugation, the radioactivity and leaked hemoglobin in the supernatant were determined. The pelleted cells were washed and extracted with isopropanol to precipitate the proteins and recover the radioactivity, cholesterol and phospholipid for analysis. Hemolysis was <4 %.

RESULTS

Reaction of cholesterol oxidase with LUV cholesterol

Representative time courses of the oxidation of cholesterol in various phospholipid LUVs are shown in Figure 1. The relative accessibility to the enzyme (RA) of the cholesterol in each LUV preparation was calculated from the initial rates of reaction according to eq. 6 in Appendix 1. RA values for 10 phospholipids are plotted as a function of LUV CMF in Figure 2. RA values were found to range over six orders of magnitude, the slowest being for DPPC LUV with a low cholesterol content and the fastest for DOPC LUV with a high cholesterol content. The fastest rates observed for DPPC at high CMF were an order of magnitude less than the lowest rate for DOPC and POPS. In all but one case, a threshold was observed at a characteristic CMF above which the cholesterol accessibility rose by ~2–4 orders of magnitude. The exception was SOPS, where oxidation rates increased linearly with CMF from an x-axis intercept close to zero.

We fitted the data in Figure 2 to a simple model described in eq. 9 (Appendix 2). For this purpose, we tested small integer stoichiometries for the apparent complexes based upon our visual inspection of these “J-curves.” Values for K_a and the relative fractions of complexed

and free sterol were then obtained by a non-linear least-squares Monte Carlo curve fitting procedure (see Appendix 2). These values were used to match theoretical curves to the data, by assuming, through trial and error, a maximal RA for the completely uncomplexed cholesterol in each phospholipid system. The resulting plots are shown in Figure 2 and the corresponding values for the four parameters are presented in Table 1. We used E/N values to gauge goodness of fit; see Appendix 2 and the legend to Figure 2. The best fitting theoretical curves were to SOPC (E/N=0.14), DMPE (E/N=0.14) and POPS (E/N=0.15); the worst fits were to DMPS)E/N=1.44).

Stoichiometries for the apparent cholesterol:phospholipid complexes of 1:1, 2:3 and 1:2 seemed plausible. We chose small integer stoichiometries rather than extracting values from least squares fits because large or non-integer stoichiometries typically suggest unrealistically large sizes for the complexes. For example, a 1.2:1 stoichiometry for cholesterol:PSM implies complexes comprised of 6 cholesterols and 5 phospholipids; other stoichiometries can give still larger and less plausible complex sizes. Nevertheless, assuming a cholesterol:phospholipid stoichiometry of 1.2:1 gave a statistically better fit for PSM than a 1:1 stoichiometry. Similarly, the fit for POPC was better with a 1:1 than a 2:3 stoichiometry, and a stoichiometry for DMPS of 2:3 worked better than a 1:1 stoichiometry

The computed association constants, K_a in Table 1, were used to show that the rise preceding the thresholds in the curves in Figure 2 was mostly due to the emergence of uncomplexed cholesterol with its elevated enzyme accessibility. The RA values for complexed cholesterol are not considered to be very accurate because the enzyme reactions were generally close to the baseline sensitivity. The RA values for uncomplexed cholesterol fell into two distinct classes: all of the di-saturated phospholipids had RA values < 50, while all the unsaturated phospholipids had RA values > 1000. From the largest RA value and the scaling factor for each phospholipid, we calculated that the highest cholesterol accessibilities reported here ranged from ~3% (for SOPC) to ~63% (for POPS) of their projected maximal values.

Equilibrium distribution of [^{14}C]cholesterol between LUVs and MBCD

This method has been used to compare the cholesterol affinities of various phospholipids (19, 24). Those studies assumed a simple partition equilibrium between two ideal compartments; that is,

$$K_p=[CP]/[P_t]/([CM]/[M_t]) \quad (1)$$

where CP is the phospholipid-associated cholesterol, P_t is total LUV phospholipid, CM is MBCD-associated cholesterol and M_t is total MBCD. However, there is evidence that both the LUVs and the cyclodextrin bind cholesterol stoichiometrically, so that the distribution reflects an equilibrium association reflecting the abundance of free rather than total reactants. In that case, assuming 1:1 stoichiometries,

$$K_e=[CP]/[P]/([CM]/[M]) \quad (2)$$

However, some of the cholesterol-phospholipid complexes appear not to be unimolecular (Table 1) and MBCD apparently binds cholesterol as a dimer (56). Affinity constants for various higher order reactions would then have different units and not be directly comparable. Finally, K_e would presumably change above the stoichiometric equivalence point; we worked at low cholesterol levels to avoid this issue.

Due to these complexities, we did not infer partition or equilibrium constants but rather expressed the equilibrium distribution of cholesterol between given LUV phospholipid and MBCD concentrations as a coefficient; namely,

$$Q=[CP]/[P_t]/([CM]/[M_t]) \quad (3)$$

(Although $Q = K_p$, these designations connote different things.) Ratios of Q values then give estimates of the distribution of cholesterol between different phospholipid compartments; this, rather than their association constants, is the parameter of interest here. Employing relatively small CMFs allowed the approximations, $[M] \approx [M_t]$ and $[P] \approx [P_t]$, so that the distribution coefficients, Q, were only a few percent smaller than the corresponding equilibrium constants, K_e, for unimolecular reactions. Except for the experiments shown in Figure 4, we also kept the proportions of the reactants constant so that $[M_t]/[P_t]$ would be the same (and [M]/[P] nearly so) for all the LUV systems, allowing their direct comparison.

Estimates of Q varied over about an order of magnitude for the phospholipids tested, with species bearing phosphorylcholine head groups and saturated acyl chains having the highest relative cholesterol affinity (Table 1). The Q values for the various phospholipids fell into high and low classes that paralleled their thermal transition temperatures (Figure 3). (We included DLPC to test a saturated phospholipid with a T_m well below the assay temperature.) Also shown in Figure 3, the Q values for most of the phospholipids were somewhat lower at 37 °C than at 25 °C. A similar phenomenon has been reported for POPC (56).

There was an additional reason to express equilibrium cholesterol distributions as Q rather than K_p values. Namely, seven high-affinity phospholipids showed a progressive ~2–4 fold increase in apparent cholesterol affinity as a function of CMF, while three weak-affinity phospholipids at low CMF did not (Figure 4). [A similar non-ideal dependence of apparent affinity on CMF has been reported for POPC (56).] The curves were not sigmoidal, suggesting that this cholesterol dependence was not cooperative. The phenomenon was observed with phospholipids with thermal transition temperatures both above and below the assay temperature (25 °C) and with DLPC, a saturated phospholipid with a T_m well bellow the assay temperature. Q values for DMPC rose up to CMF ~0.2 and fell two-fold thereafter; other Q values seemed to approach a plateau at high CMF.

Characterization of RBC membrane cholesterol

We also measured the accessibility to cholesterol oxidase of cholesterol in the membranes of intact human erythrocytes after increasing their sterol concentration by equilibration with MBCD-cholesterol. To avoid hemolysis, we did not deplete the cells of cholesterol. The results are given in Figure 2 and Table 1. The parameters for red cells resembled those for the saturated phosphorylcholine systems. We also determined the distribution of cholesterol between the red cells and MBCD. The Q value is presented in Table 1 as 11. This figure presumably underestimates their cholesterol affinity, because their high content of cholesterol makes $[P] \ll [P_t]$. The K_e for the RBC, estimated to be 19, is therefore a more appropriate value for comparison to the Q values for the LUVs.

DISCUSSION

Considerable scatter was encountered in the data for the relative accessibility of cholesterol to cholesterol oxidase because each calculation entailed dividing the initial rate of reaction by the concentrations of phospholipids, cholesterol and the enzyme (the activity of which might vary over time). Furthermore, each curve contained points from multiple experiments

gathered over a period of months. The interpretation of the data is, of course, model-dependent; however, the simplest and most appropriate formulation we know of postulates that bilayer cholesterol is in a stoichiometric association equilibrium with the phospholipids (Appendix 2). While the RA data were reasonably well fit by a Monte Carlo least-squares analysis, the values we inferred should not be considered to be precise. Nevertheless, they provide novel and useful information regarding cholesterol-phospholipid associations and the use of cholesterol oxidase and β-cyclodextrins as probes, as follows.

1) Relative accessibilities

In keeping with earlier reports, the reaction of cholesterol with cholesterol oxidase varied greatly from one phospholipid environment to another and rose dramatically when LUV cholesterol was incremented above a threshold (32, 40, 45, 46, 57). Polar head group species did not seem to exert a strong influence; in contrast, the RA values above threshold were orders of magnitude greater for unsaturated than saturated chains. The large differences in enzyme kinetics among the LUVs probably do not represent variations in K_d, the disassociation constant for the binding of cholesterol oxidase, given that (a) the enzyme binds superficially to the surface of the vesicles; (b) the K_d is rather insensitive to vesicle composition; and (c) the various phosphorylcholine phospholipids should bind the enzyme similarly yet had widely divergent RA values (38, 42, 43).

It seems more likely that the rate of the cholesterol oxidase reactions reflected the fractional occupancy of the binding pocket of the bound enzyme by its substrate. This, in turn, should be constrained to some degree by the free energy change associated with the partition of the substrate between the bilayer and the active site; hence, the strength of cholesterol-phospholipid associations (38, 42, 58). However, the thermodynamic stability of cholesterol-phospholipid associations may not be the major factor limiting the cholesterol oxidase reactions, given that the RA values for both complexed and uncomplexed cholesterol varied over several orders of magnitude for the various phospholipids while their cholesterol affinities (Q values) only varied by about ten-fold. We therefore imagine that a cholesterol molecule held in the bilayer with a given affinity might nevertheless assume a variety of dispositions that strongly affect its exposure at the aqueous interface. This could also explain why the rates of exit of cholesterol from different phospholipid vesicles have a much larger spread than their corresponding sterol affinities (59). Other sterol-directed proteins might similarly sense the subtleties of sterol presentation reported by cholesterol oxidase.

The fact that the oxidation rates varied by orders of magnitude above the thresholds of the various phospholipids suggests that the uncomplexed sterol is not at all free of their specific influences. Rather, the “free” cholesterol seems to be constrained by interactions similar to those experienced by the complexed molecules in that bilayer, albeit to a far smaller degree. This premise seems reasonable, given that the complexed and uncomplexed sterol molecules both reside in the same phospholipid environment. It is important to note that the factors that determine the velocities of the enzyme reaction should not affect the values we obtained for cholesterol-phospholipid stoichiometries and affinities, discussed below.

2) Stoichiometries

While not definitive, the cholesterol dependence J-curves in Figure 2 were consistent with small integer stoichiometries for cholesterol:phospholipid associations of ≈ 1:1, 2:3 and 1:2 mol/mol. These values are in fair agreement with those reported for perfringolysin O binding, the rate of sterol transfer from bilayers to β-cyclodextrin and the visualization of phase coexistence as well as average molecular area measurements on mixed monolayers (26, 27, 29, 32–36). Introducing oligomerization of the complexes in our model did not improve the fits to the data.

We considered some alternative explanations of the observed threshold behavior. Lateral phase heterogeneity would not occur in these bilayer systems, given that they should be homogeneous liquids at 37 °C (23, 60, 61). [But see ref. (62).] Furthermore, the Michaelis, dissociation and catalytic constants (K_m, K_d and k_{cat}) of the enzyme should not vary with the cholesterol content of the bilayer (38, 39, 42, 43). We also considered whether the observed thresholds might reflect the limited solubility of the cholesterol, since sterols in excess of a sharp threshold form crystals in phospholipid bilayers (61). However, the thresholds for all the phosphatidylcholines occurred at cholesterol concentrations significantly below the well-documented solubility limit of CMF = 0.66 (61). In addition, we found that POPC and DOPC had lower thresholds than DPPC and DMPC, while the solubility limit (head group “umbrella coverage”) for cholesterol in all phosphatidylcholine bilayers is thought to be the same (61). Finally, crystallization is unlikely to cause the enhanced accessibility of super-threshold cholesterol observed with the probes, cholesterol oxidase and perfringolysin O.

3) Stability of complexes

The K_a values in Table 1 are the first to quantify the strength of the association of cholesterol with relevant bilayer phospholipids, previous studies giving only relative affinities; e.g., ref. 19 and 24. The Ka values for complexes with different stoichiometries cannot be directly compared, because they define different orders of reaction and, therefore, have different units. However, the calculated values for the fraction of cholesterol free at its equivalence point offers a comparison of the stabilities of all of the phospholipid complexes. These estimates suggest that on the order of 80–98% of the bilayer cholesterol would be complexed at the equivalence points of each of these phospholipids, with saturated phospholipids having the least free cholesterol at that point (Table 1). An implication of these results is that the sterol in eukaryotic plasma membranes (and perhaps others) mostly resides in phospholipid complexes.

SOPS was the exception

It showed no apparent threshold in the cholesterol dependence of cholesterol oxidase reaction rates; hence, no evidence for complex formation. This inference is supported by the high accessibility of the cholesterol in SOPS LUVs; its RA exceeded all other phospholipids at CMF <0.2 where complexation should be the strongest (Figure 2). The fact that SOPS had a lower relative accessibility to cholesterol oxidase than did DOPC at high CMF is consistent with the premise, mentioned above, that the activity of uncomplexed sterol molecules is constrained by their bilayer environment in a phospholipid-specific fashion. SOPS is a major phospholipid in biological membranes, where it might have the effect of lowering (by dilution) the overall threshold of the bilayer in which it resides; *i.e.*, the CMF at the bend of the J-curve for cholesterol activation. Any number of other, unexamined phospholipids could behave similarly.

4) Q values

The equilibrium distribution of cholesterol between LUVs and MBCD provided a measure of the relative affinity of cholesterol for the various phospholipids (Table 1). The results are in accord with and extend reports in the literature (19, 24, 56, 60, 63). The saturated phospholipids tested generally had a higher cholesterol affinity than the unsaturated species, just as indicated by cholesterol oxidase accessibility (see Table 1 and Figure 3). The low Q value for SOPS is consistent with the cholesterol oxidase data suggesting a weak affinity for cholesterol. Why SOPS had no threshold (Figure 2) yet showed a rising Q value (Figure 4) is worthy of investigation.

The Q values describe the distribution of cholesterol between different LUVs and a reference sink (MBCD) and thereby provide a comparison of the cholesterol affinities of the various phospholipids (19, 24). In contrast, K_a values describe the association equilibrium of cholesterol between its phospholipid complexes and its uncomplexed form in the same bilayer. Thus, the two parameters need not agree. However, as shown in Table 1, the span of the K_a values for phospholipids making ~1:1 complexes (namely, 32-fold) resembles that of their Q values (namely, 15-fold). Indeed, the K_a and Q values for these six ~1:1 species are well correlated; namely, $R^2 = 0.77$. Furthermore, the values in Table 1 for Ka, the RA of uncomplexed cholesterol, the percent of cholesterol free of complexes at the stoichiometric equivalence point and the Q values are in good mutual agreement with respect to the relative strengths of association of bilayer cholesterol with the various phospholipids (Figure 5).

These data bear on the question of whether the distribution of cholesterol among cellular membranes is driven by an association equilibrium with their constituent phospholipids. Key factors would then be the relative abundance of the different phospholipids species in each compartment, the relative stability of their cholesterol complexes and their complexation stoichiometries, above which cholesterol affinity would fall. While much more quantitative lipidomic data on purified organelles is needed, we know that plasma membrane bilayers are rich in sphingolipids, phosphatidylcholines and phosphatidylserines bearing saturated alkyl chains, while the non-endocytic cytoplasmic membrane phospholipids have more unsaturated fatty acid chains and polar head groups other than phosphorylcholine and phosphorylserine (1, 2). Indeed, the cholesterol:phospholipid ratio in plasma membranes is typically close to 0.8 (*i.e.*, CMF = 0.44), matching the threshold stoichiometry of the high affinity plasma membrane-type phospholipids shown in Table 1; see also ref. (16). In the case of cultured human fibroblasts, the plasma membrane contains approximately 80% of the cell cholesterol and 50% of the phospholipid phosphorus (64, 65). The endocytic pathway might contain another 10% of the cell cholesterol through its traffic with the plasma membrane, leaving ~10% of the cholesterol in the other cytoplasmic membrane compartments. Thus, the ~5–10 fold difference in the cholesterol:phospholipid ratio of the fibroblast plasma membranes and cytoplasmic membranes is consistent with the relative affinity and abundance of the phospholipids in those compartments; see Table 1 and ref. (1, 19, 24). Passive equilibration of cholesterol among the organelle phospholipid bilayers is also consistent with the lack of evidence for energized cholesterol pumping by any of the transfer proteins identified thus far (10–12, 15).

With regard to cholesterol homeostasis, our data support the following scenario (13). Cholesterol would tend to accumulate as phospholipid complexes in the various bilayer compartments up to their stoichiometric equivalence points. Cholesterol above those thresholds would increasingly exit, as has been reported (29, 32, 34). Once the large pool of high-affinity, high-threshold phospholipids in the plasma membrane is complexed, further increments in cholesterol will increasingly partition to the cytoplasmic membranes. Their cholesterol affinity is relatively low and will diminish as their low complexing thresholds are exceeded. When the cholesterol in the ER bilayer passes its equivalence point, the excess low-affinity sterol will become available to and activate resident homeostatic proteins. These effectors will then mediate the down regulation of cell cholesterol accretion (13). A parallel mechanism occurs in mitochondria. There, excess cholesterol is converted to 27-hydroxycholesterol, a manifold feedback inhibitor of cholesterol accretion (13). In this scenario, therefore, the steady-state distribution of cell cholesterol will depend in a complex but precise manner on the magnitude of the phospholipid compartments of the diverse organelles, their net cholesterol thresholds and their relative cholesterol affinities both below and above those thresholds.

There is analytical and functional evidence that the cholesterol in not only the plasma membranes, but in the ER and mitochondria as well, normally resides at a threshold in keeping with the homeostatic feedback mechanism described above (8, 13, 32, 63, 67). The threshold for ER cholesterol has been reported to be ~0.05 moles/mole phospholipid, far below any stoichiometric equivalence point thus far reported; see Results and ref. (8, 13, 35–37, 63). It is implausible that this stoichiometry represents complexes composed of 19 phospholipids and one cholesterol. Instead, certain ER phospholipids, like SOPS, might bind cholesterol very weakly or not form cholesterol complexes at all, so that they will reduce the overall equivalence point of that bilayer. Alternatively, the presence of intercalating amphiphile(s) that bind to phospholipids could reduce the ER threshold by displacing cholesterol (55–57).

Finally, to test the biological relevance of this characterization of cholesterol-phospholipid interactions, we examined human red blood cell membranes. As seen in Table 1, the cholesterol oxidase accessibility of cholesterol in intact red cells closely resembled the saturated phosphorylcholine phospholipid LUVs in their 1:1 threshold, their high K_a values, the low RA of their cholesterol both below and above their threshold and in the fraction of cholesterol free at the threshold. These data are in accord with the abundance of phospholipids with saturated chains and phosphorylcholine head groups in the outer leaflet of the RBC bilayer (66–68). The relatively high cholesterol oxidase sensitivity of the cytoplasmic leaflet of this membrane (not tested here) also agrees with its phospholipid composition (41, 69–71). The apparent Q value for the RBC (namely, 11) was lower than that predicted from the sum of the phospholipids at their outer and inner leaflets. However, one should use K_e rather than Q for this estimate, since the high cholesterol in this system makes [P] significantly smaller than [P_t]. The value obtained for K_e, 19, scales with the Q values for PSM and DPPC (Table 1).

These results bear on how the level of cholesterol in RBCs is maintained over their ~4 months in circulation, given that these cells lack the homeostatic elements mentioned above. The pool of cholesterol in RBCs is not static but exchanges with the plasma lipoproteins on a timescale of hours (72). Nevertheless, human red cell membrane cholesterol rests at stoichiometric equivalence with its phospholipids, as evidenced by the thresholds in both its susceptibility to cholesterol oxidase and its rate of transfer to MBCD; see Figure 2 and refs. (32, 57). It seems plausible that RBC bilayer cholesterol is maintained at its equivalence point by passive equilibration with the plasma lipoproteins. If so, it could be the chemical activity of cholesterol in the plasma lipoproteins is itself set physiologically to maintain the level of red cell cholesterol membrane (and perhaps plasma membranes in general) at their equivalence points. How this might occur is not known.

Acknowledgments

The authors are grateful to Karl Freed (University of Chicago), Arun Radhakrishnan (University of Texas Southwestern Medical Center) and Heiko Heerklotz (University of Toronto) for their valuable comments on this manuscript.

Abbreviations

For a list of the symbols used in the equations, see Appendix 3

BSA	bovine serum albumin
CH	cholesterol

CMF	bilayer cholesterol mole fraction (*i.e.*, moles cholesterol/(moles cholesterol + moles phospholipid)
DLPC	1,2-dilauroyl-2-oleoyl-sn-glycero-3-phosphatidylcholine
DMPC	1,2-myristoyl-2-oleoyl-sn-glycero-3-phosphatidylcholine
DMPE	1,2-myristoyl-2-oleoyl-sn-glycero-3-phosphatidylethanolamine
DMPS	1,2-myristoyl-2-oleoyl-sn-glycero-3-phosphatidylserine
DOPC	1,2-dioleoyl-sn-glycero-3-phosphatidylcholine
DPPC	1,2-dipalmitoyl-2-oleoyl-sn-glycero-3-phosphatidylcholine
ER	endoplasmic reticulum
HBS	150 mM NaCl plus 5 mM Hepes-NaOH, pH 7.4
LUV	large unilamellar vesicles
MBCD	methyl-β-cyclodextrin
POPC	1-palmitoyl-2-oleoyl-sn-glycero-3-phosphatidylcholine
POPS	1-palmitoyl-2-oleoyl-sn-glycero-3-phosphatidylserine
PSM	N-palmitoyl-D-erythro-sphingosylphosphorylcholine
RA	relative cholesterol accessibility
RBC	red blood cell
SOPS	1-stearoyl-2-oleoyl-sn-glycero-3-phosphatidylserine
SOPC	1-stearoyl-2-oleoyl-sn-glycero-3-phosphatidylcholine.

References

1. van Meer G, Voelker DR, Feigenson GW. Membrane lipids: where they are and how they behave. Nat Rev Mol Cell Biol. 2008; 9:112–124. [PubMed: 18216768]
2. Andreyev AY, Fahy E, Guan Z, Kelly S, Li X, McDonald JG, Milne S, Myers D, Park H, Ryan A, Thompson BM, Wang E, Zhao Y, Brown HA, Merrill AH, Raetz CR, Russell DW, Subramaniam S, Dennis EA. Subcellular organelle lipidomics in TLR-4-activated macrophages. J Lipid Res. 2010; 51:2785–2797. [PubMed: 20574076]
3. Phillips, MC. The physical state of phospholipids and cholesterol in monolayers, bilayers, and membranes. In: Danielli, JF.; Rosenberg, MD.; Cadenhead, DA., editors. Progress in Surface and Membrane Science. Academic Press; New York: 1972. p. 139-221.
4. Ohvo-Rekila H, Ramstedt B, Leppimaki P, Slotte JP. Cholesterol interactions with phospholipids in membranes. Prog Lipid Res. 2002; 41:66–97. [PubMed: 11694269]
5. Hung WC, Lee MT, Chen FY, Huang HW. The condensing effect of cholesterol in lipid bilayers. Biophys J. 2007; 92:3960–3967. [PubMed: 17369407]
6. Yeagle PL. Cholesterol and the Cell-Membrane. Biochimica Et Biophysica Acta. 1985; 822:267–287. [PubMed: 3904832]
7. Miao L, Nielsen M, Thewalt J, Ipsen JH, Bloom M, Zuckermann MJ, Mouritsen OG. From Lanosterol to Cholesterol: Structural Evolution and Differential Effects on Lipid Bilayers. Biophys J. 2002; 82:1429–1444. [PubMed: 11867458]
8. Radhakrishnan A, Goldstein JL, McDonald JG, Brown MS. Switch-like Control of SREBP-2 Transport Triggered by Small Changes in ER Cholesterol: A Delicate Balance. Cell Metabolism. 2008; 8:512–521. [PubMed: 19041766]
9. Lange Y, Ye J, Rigney M, Steck TL. Regulation of endoplasmic reticulum cholesterol by plasma membrane cholesterol. J Lipid Res. 1999; 40:2264–2270. [PubMed: 10588952]

10. Mesmin B, Maxfield FR. Intracellular sterol dynamics. Biochimica et Biophysica Acta (BBA) - Molecular and Cell Biology of Lipids. 2009; 1791:636–645.
11. Prinz WA. Lipid Trafficking sans Vesicles: Where, Why, How? Cell. 2010; 143:870–874. [PubMed: 21145454]
12. Ikonen E. Cellular cholesterol trafficking and compartmentalization. Nat Rev Mol Cell Biol. 2008; 9:125–138. [PubMed: 18216769]
13. Steck TL, Lange Y. Cell cholesterol homeostasis: Mediation by active cholesterol. Trends in Cell Biology. 2010; 20:680–687. [PubMed: 20843692]
14. Wattenberg BW, Silbert DF. Sterol partitioning among intracellular membranes. Testing a model for cellular sterol distribution. J Biol Chem. 1983; 258:2284–2289. [PubMed: 6822559]
15. Maxfield FR, van Meer G. Cholesterol, the central lipid of mammalian cells. Curr Opin Cell Biol. 2010
16. Lange Y, Steck TL. Cholesterol homeostasis and the escape tendency (activity) of plasma membrane cholesterol. Prog Lipid Res. 2008; 47:319–332. [PubMed: 18423408]
17. Silvius JR. Role of cholesterol in lipid raft formation: lessons from lipid model systems. Biochim Biophys Acta. 2003; 1610:174–183. [PubMed: 12648772]
18. Silvius JR. Partitioning of membrane molecules between raft and non-raft domains: Insights from model-membrane studies. Biochimica et Biophysica Acta (BBA) - Molecular Cell Research. 2005; 1746:193–202.
19. Niu SL, Litman BJ. Determination of membrane cholesterol partition coefficient using a lipid vesicle-cyclodextrin binary system: effect of phospholipid acyl chain unsaturation and headgroup composition. Biophys J. 2002; 83:3408–3415. [PubMed: 12496107]
20. Quinn PJ. Lipid-lipid interactions in bilayer membranes: married couples and casual liaisons. Prog Lipid Res. 2012; 51:179–198. [PubMed: 22342933]
21. Ramstedt B, Slotte JP. Interaction of cholesterol with sphingomyelins and acyl-chain-matched phosphatidylcholines: A comparative study of the effect of the chain length. Biophysical Journal. 1999; 76:908–915. [PubMed: 9929492]
22. Berkowitz ML. Detailed molecular dynamics simulations of model biological membranes containing cholesterol. Biochim Biophys Acta. 2009; 1788:86–96. [PubMed: 18930019]
23. Mannock DA, Lewis R, McMullen TPW, McElhaney RN. The effect of variations in phospholipid and sterol structure on the nature of lipid-sterol interactions in lipid bilayer model membranes. Chemistry and Physics of Lipids. 2010; 163:403–448. [PubMed: 20371224]
24. Leventis R, Silvius JR. Use of cyclodextrins to monitor transbilayer movement and differential lipid affinities of cholesterol. Biophys J. 2001; 81:2257–2267. [PubMed: 11566796]
25. Keller SL, Radhakrishnan A, McConnell HM. Saturated phospholipids with high melting temperatures form complexes with cholesterol in monolayers. Journal of Physical Chemistry B. 2000; 104:7522–7527.
26. McConnell HM, Radhakrishnan A. Condensed complexes of cholesterol and phospholipids. Biochim Biophys Acta. 2003; 1610:159–173. [PubMed: 12648771]
27. Radhakrishnan A, McConnell HM. Condensed complexes of cholesterol and phospholipids. Biophys J. 1999; 77:1507–1517. [PubMed: 10465761]
28. McConnell HM, Vrljic M. Liquid-liquid immiscibility in membranes. Annu Rev Biophys Biomol Struct. 2003; 32:469–492. [PubMed: 12574063]
29. Radhakrishnan A, McConnell HM. Chemical activity of cholesterol in membranes. Biochemistry. 2000; 39:8119–8124. [PubMed: 10889017]
30. Ratajczak MK, Chi EY, Frey SL, Cao KD, Luther LM, Lee KYC, Majewski J, Kjaer K. Ordered Nanoclusters in Lipid-Cholesterol Membranes. Physical Review Letters. 2009; 103
31. Kessel A, Ben-Tal N, May S. Interactions of Cholesterol with Lipid Bilayers: The Preferred Configuration and Fluctuations. Biophysical Journal. 2001; 81:643–658. [PubMed: 11463613]
32. Lange Y, Ye J, Steck TL. How cholesterol homeostasis is regulated by plasma membrane cholesterol in excess of phospholipids. Proc Natl Acad Sci U S A. 2004; 101:11664–11667. [PubMed: 15289597]

33. Ohvo H, Slotte JP. Cyclodextrin-mediated removal of sterols from monolayers: effects of sterol structure and phospholipids on desorption rate. Biochemistry. 1996; 35:8018–8024. [PubMed: 8672506]
34. Radhakrishnan A, McConnell HM. Thermal Dissociation of Condensed Complexes of Cholesterol and Phospholipid. The Journal of Physical Chemistry B. 2002; 106:4755–4762.
35. Johnson BB, Moe PC, Wang D, Rossi K, Trigatti BL, Heuck AP. Modifications in Perfringolysin O Domain 4 Alter the Cholesterol Concentration Threshold Required for Binding. Biochemistry. 2012
36. Flanagan JJ, Tweten RK, Johnson AE, Heuck AP. Cholesterol Exposure at the Membrane Surface Is Necessary and Sufficient to Trigger Perfringolysin O Binding. Biochemistry. 2009; 48:3977–3987. [PubMed: 19292457]
37. Das A, Goldstein JL, Anderson DD, Brown MS, Radhakrishnan A. Use of mutant 125I-Perfringolysin O to probe transport and organization of cholesterol in membranes of animal cells. Proceedings of the National Academy of Sciences. 2013
38. Kreit J, Sampson NS. Cholesterol oxidase: physiological functions. FEBS J. 2009; 276:6844–6856. [PubMed: 19843168]
39. Slotte JP. Enzyme-Catalyzed Oxidation of Cholesterol in Pure Monolayers at the Air-Water-Interface. Biochimica Et Biophysica Acta. 1992; 1123:326–333. [PubMed: 1536872]
40. Patzer EJ, Wagner RR, Barenholz Y. Cholesterol oxidase as a probe for studying membrane organisation. Nature. 1978; 274:394–395. [PubMed: 209332]
41. Thurnhofer H, Gains N, Mutsch B, Hauser H. Cholesterol Oxidase as a Structural Probe of Biological-Membranes - Its Application to Brush-Border Membrane. Biochimica Et Biophysica Acta. 1986; 856:174–181. [PubMed: 3456800]
42. Ahn KW, Sampson NS. Cholesterol oxidase senses subtle changes in lipid bilayer structure. Biochemistry. 2004; 43:827–836. [PubMed: 14730988]
43. Chen X, Wolfgang DE, Sampson NS. Use of the parallax-quench method to determine the position of the active-site loop of cholesterol oxidase in lipid bilayers. Biochemistry. 2000; 39:13383–13389. [PubMed: 11063575]
44. Mattjus P, Slotte JP. Availability for Enzyme-Catalyzed Oxidation of Cholesterol in Mixed Monolayers Containing Both Phosphatidylcholine and Sphingomyelin. Chemistry and Physics of Lipids. 1994; 71:73–81. [PubMed: 8039259]
45. Slotte JP. Enzyme-Catalyzed Oxidation of Cholesterol in Mixed Phospholipid Monolayers Reveals the Stoichiometry at Which Free-Cholesterol Clusters Disappear. Biochemistry. 1992; 31:5472–5477. [PubMed: 1610794]
46. Ali MR, Cheng KH, Huang J. Assess the nature of cholesterol-lipid interactions through the chemical potential of cholesterol in phosphatidylcholine bilayers. Proc Natl Acad Sci U S A. 2007; 104:5372–5377. [PubMed: 17372226]
47. Mattjus P, Hedstrom G, Slotte JP. Monolayer interaction of cholesterol with phosphatidylcholines: effects of phospholipid acyl chain length. Chemistry and Physics of Lipids. 1994; 74:195–203.
48. Lange Y, Ye J, Duban ME, Steck TL. Activation of membrane cholesterol by 63 amphipaths. Biochemistry. 2009; 48:8505–8515. [PubMed: 19655814]
49. Lange Y, Ye J, Steck TL. Activation of membrane cholesterol by displacement from phospholipids. J Biol Chem. 2005; 280:36126–36131. [PubMed: 16129675]
50. Ratajczak MK, Ko YTC, Lange Y, Steck TL, Lee KYC. Cholesterol Displacement from Membrane Phospholipids by Hexadecanol. Biophys J. 2007; 93:2038–2047. [PubMed: 17526582]
51. Macdonald RC, Macdonald RI, Menco BPM, Takeshita K, Subbarao NK, Hu LR. Small-Volume Extrusion Apparatus for Preparation of Large, Unilamellar Vesicles. Biochimica Et Biophysica Acta. 1991; 1061:297–303. [PubMed: 1998698]
52. Steck TL, Kant JA. Preparation of impermeable ghosts and inside-out vesicles from human erythrocyte membranes. Methods Enzymol. 1974; 31:172–180. [PubMed: 4370662]
53. Lange Y, Echevarria F, Steck TL. Movement of zymosterol, a precursor of cholesterol, among three membranes in human fibroblasts. J Biol Chem. 1991; 266:21439–21443. [PubMed: 1939176]

54. Chen PS, Toribara TY, Warner H. Microdetermination of Phosphorus. Anal Chem. 1956; 28:1756–1758.
55. Steck TL, Lange Y. How slow is the transbilayer diffusion (flip-flop) of cholesterol? Biophys J. 2012; 102:945–946. [PubMed: 22385866]
56. Tsamaloukas AD, Szadkowska H, Slotte PJ, Heerklotz HH. Interactions of cholesterol with lipid membranes and cyclodextrin characterized by calorimetry. Biophys J. 2005; 89:1109–1119. [PubMed: 15923231]
57. Lange Y, Cutler HB, Steck TL. The effect of cholesterol and other intercalated amphipaths on the contour and stability of the isolated red cell membrane. J Biol Chem. 1980; 255:9331–9337. [PubMed: 7410427]
58. Sampson NS, Vrielink A. Cholesterol oxidases: A study of nature's approach to protein design. Accounts Chem Res. 2003; 36:713–722.
59. Lundkatz S, Laboda HM, Mclean LR, Phillips MC. Influence of Molecular Packing and Phospholipid Type on Rates of Cholesterol Exchange. Biochemistry. 1988; 27:3416–3423. [PubMed: 3390441]
60. Feigenson GW. Phase boundaries and biological membranes. Annu Rev Bioph Biom. 2007; 36:63–77.
61. Huang J, Buboltz JT, Feigenson GW. Maximum solubility of cholesterol in phosphatidylcholine and phosphatidylethanolamine bilayers. Biochim Biophys Acta. 1999; 1417:89–100. [PubMed: 10076038]
62. Heerklotz H, Tsamaloukas A. Gradual change or phase transition: characterizing fluid lipid-cholesterol membranes on the basis of thermal volume changes. Biophys J. 2006; 91:600–607. [PubMed: 16632513]
63. Yeagle PL, Young JE. Factors Contributing to the Distribution of Cholesterol among Phospholipid-Vesicles. Journal of Biological Chemistry. 1986; 261:8175–8181. [PubMed: 3722148]
64. Lange Y, Swaisgood MH, Ramos BV, Steck TL. Plasma membranes contain half the phospholipid and 90% of the cholesterol and sphingomyelin in cultured human fibroblasts. J Biol Chem. 1989; 264:3786–3793. [PubMed: 2917977]
65. Lange Y, Ye J, Steck TL. Activation mobilizes the cholesterol in the late endosomes-lysosomes of niemann pick type C cells. PLoS One. 2012; 7:e30051. [PubMed: 22276143]
66. Virtanen JA, Cheng KH, Somerharju P. Phospholipid composition of the mammalian red cell membrane can be rationalized by a superlattice model. Proceedings of the National Academy of Sciences of the United States of America. 1998; 95:4964–4969. [PubMed: 9560211]
67. van Golde LMG, Tomasi V, van Deenen LLM. Determination of molecular species of lecithin from erythrocytes and plasma. Chemistry and Physics of Lipids. 1967; 1:282–293.
68. Hullin F, Bossant MJ, Salem N Jr. Aminophospholipid molecular species asymmetry in the human erythrocyte plasma membrane. Biochim Biophys Acta. 1991; 1061:15–25. [PubMed: 1995054]
69. Gottlieb MH. The reactivity of human erythrocyte membrane cholesterol with a cholesterol oxidase. Biochim Biophys Acta. 1977; 466:422–428. [PubMed: 857889]
70. Lange Y, Matthies H, Steck TL. Cholesterol oxidase susceptibility of the red cell membrane. Biochim Biophys Acta. 1984; 769:551–562. [PubMed: 6421320]
71. Lange Y, Ye J, Steck TL. Scrambling of phospholipids activates red cell membrane cholesterol. Biochemistry. 2007; 46:2233–2238. [PubMed: 17269796]
72. Cooper RA, Arner EC, Wiley JS, Shattil SJ. Modification of red cell membrane structure by cholesterol-rich lipid dispersions. A model for the primary spur cell defect. J Clin Invest. 1975; 55:115–126. [PubMed: 162782]

APPENDICES

Appendix 1. Analysis of cholesterol oxidase data

To estimate the relative accessibility of bilayer cholesterol in each cholesterol oxidase assay, we assumed a simple rate expression for the reaction: $v = E_e\, k_{cat}\, C_a/(C_a + K_m)$, where v is

the initial velocity of the enzyme reaction (in μmoles/min), E_e is the effective (*i.e.*, membrane associated) fraction of the total enzyme (E_t), K_m is the Michaelis constant and C_a is the bilayer cholesterol available to the enzyme (all in μmoles). k_{cat} is the first order rate constant for the catalytic step (min^{-1}). Since the cholesterol concentration was well below the K_m for the cholesterol oxidase, the velocity of the reaction was assumed to vary directly with its availability, C_a (42). In that case, $v \approx E_e\, k_{cat}\, C_a / K_m$. In addition, the effective enzyme concentration, E_e, is a minor fraction of total cholesterol oxidase. Under our conditions, the abundance of these enzyme-bilayer complexes is far below their dissociation constant, K_d (42). Consequently, the effective enzyme concentration is given by $E_e \approx E_t\, P_t / K_d$, where P_t is the total phospholipid concentration. Thus,

$$v \cong k_{cat}\, E_t\, P_t\, C_a/(K_d\, K_m) \quad (4)$$

Since k_{cat}, K_d and K_m are assumed not to vary under our experimental conditions,

$$v \propto E_t\, P_t\, C_a \quad (5)$$

Hence, $C_a \propto v / (E_t\, P_t)$. The relative fraction of total LUV cholesterol accessible to the enzyme, $RA = C_a / C_t$, was therefore estimated as

$$RA \propto v/(E_t\, P_t\, C_t) \quad (6)$$

Appendix 2. Analysis of cholesterol oxidase data

We assumed an ideal equilibrium association reaction between cholesterol (C) and phospholipids (P) as

$$n\,C + m\,P \leftrightarrow C_n{-}P_m \quad (7)$$

$$K_a = [C_n P_m]/[C]^n\,[P]^m \quad (8)$$

where n/m denotes the stoichiometry of a given complex and K_a is its association constant. The relative accessibility of the cholesterol to cholesterol oxidase in a given system is then

$$RA = q\,n\,[C_n P_m] + r\,[C] \quad (9)$$

where q and r are, respectively, the fractional accessibilities of the cholesterol in the complexed and uncomplexed states. We fitted the data in Figure 2 using equations 7–9, assigning various small integer stoichiometries and iterating values for K_a, q and r in a Markovian Monte Carlo scheme such that the cost function, E, converged to a minimum. E is the sum of the squares of the differences between the logs of data points and the logs of the corresponding fits. Goodness of fit is E/N, where N is the number of data points in the curve. Using logs of the values made the comparisons independent of the scale of RA and gave better fits at the bend in the curves (sensitive indicators of K_a). Low E/N values signify better fits. The calculated best fit values were scaled to the data by multiplying them by an empirical factor that should correspond to the RA of the completely uncomplexed cholesterol in each phospholipid system.

Appendix 3. Symbols used

C	cholesterol (see eq. 7–9)
C_a	LUV cholesterol available to the enzyme (see eq. 4–5)
CM	cholesterol-MBCD complex (see eq. 2)
CP	cholesterol-phospholipid complex (see eq. 2)
C_t	total cholesterol (see eq. 6)
E_e	effective enzyme concentration; *i.e.*, bound to LUV
E_t	total enzyme concentration (see eq. 4)
K_a	association constant for cholesterol-phospholipid association (see eq. 8)
k_{cat}	first order rate constant for the cholesterol oxidase reaction
K_d	dissociation constant for the cholesterol oxidase-LUV binding reaction
K_e	equilibrium constant for the cholesterol equilibrium between LUVs and MBCD (see eq. 2)
K_m	Michaelis constant
K_p	partition coefficient for the cholesterol equilibrium between LUVs and MBCD (see eq. 1)
m	stoichiometry of phospholipid complexed with phospholipid (see eq. 7)
M_t	total MBCD (see eq. 3)
n	stoichiometry of cholesterol complexed with phospholipid (see eq. 7)
P	phospholipid (see eq. 2)
P_t	total phospholipid (see eq. 3)
Q	cholesterol equilibrium distribution coefficient = $[CP]/[P_t]/([CM]/[M_t])$ (see eq. 3)
q	theoretical fractional accessibility of cholesterol in complexes (see eq. 9)
r	theoretical fractional accessibility of free cholesterol (see eq. 9)

RA relative accessibility of cholesterol in cholesterol oxidase experiments (see eq. 6)

v initial velocity of cholesterol oxidase reactions (μmoles/min)

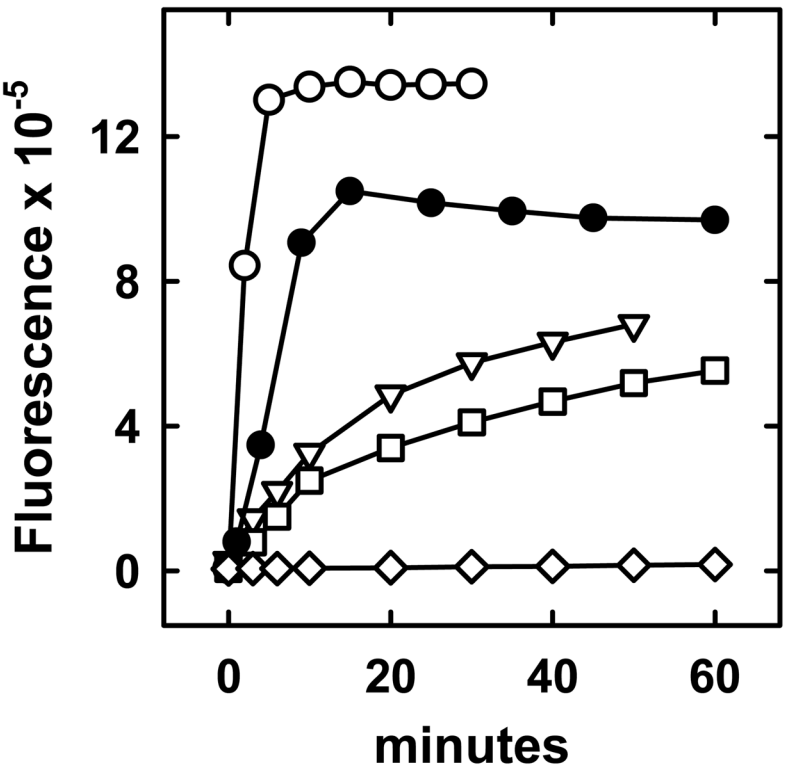

Figure 1.

Examples of time courses of oxidation of LUV cholesterol. LUV phospholipid (PL), cholesterol mole fraction (CMF) and cholesterol oxidase (CO) were varied as follows. POPC (PL = 0.62 mM, CMF = 0.43, CO = 1 U/ml), (○); DOPC (PL = 0.71 mM, CMF = 0.26, CO = 0.04 U/ml), (●); PSM (PL = 0.25 mM, CMF = 0.61, CO = 10 U/ml), (▽); DMPC (PL = 0.40 mM, CMF = 0.52, CO = 2 U/ml), (□); Minus LUVs (CO = 2 U/ml), (◇).

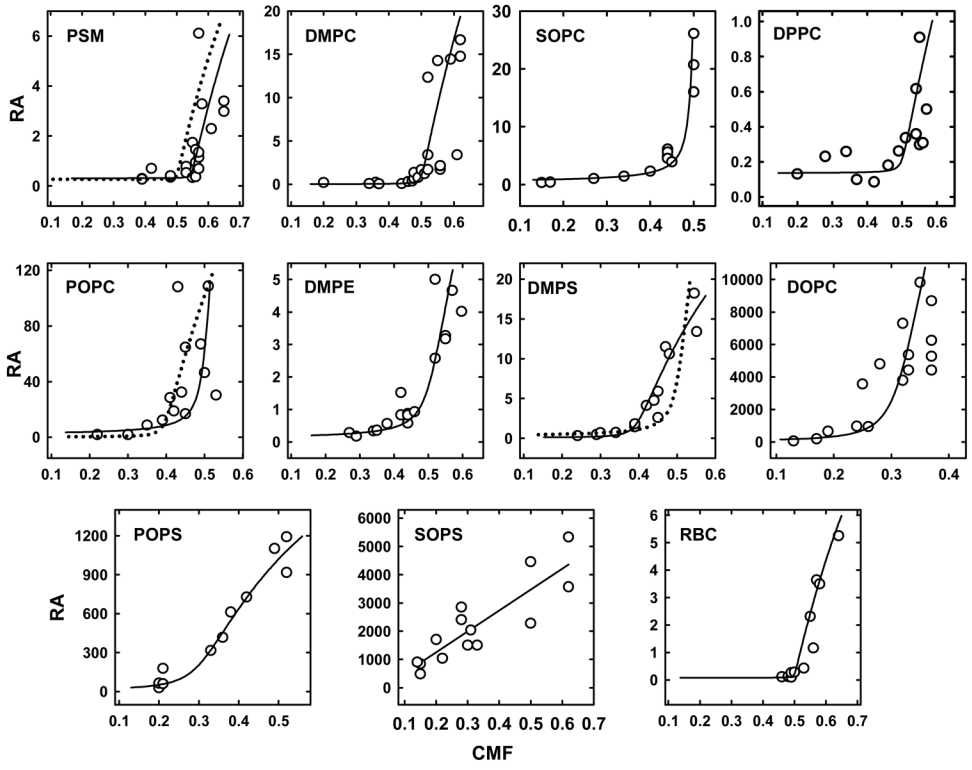

Figure 2.

Dependence of the relative accessibility (RA) of cholesterol to cholesterol oxidase on membrane cholesterol. CMF, cholesterol mole fraction. [Data points are in arbitrary units calculated according to eq. (6) in Appendix 1]. Solid lines, best fits using the values given in Table 1, columns a-d; however, the calculated curve for DPPC had 0.1 unit added to the baseline. The dotted line for PSM was obtained by assuming a stoichiometry of 1:1; its goodness of fit E/N value was 1.17, clearly less good than E/N = 0.41 for a 1.2:1 stoichiometry. The dotted line for POPC tested a stoichiometry of 2:3; its E/N value was 1.84, clearly not as good as the E/N = 0.80 for a 1:1 stoichiometry. The dotted line for DMPS tested a stoichiometry of 1:1; its E/N value was 2.00, not as good as the E/N = 1.44 for a 2:3 stoichiometry.

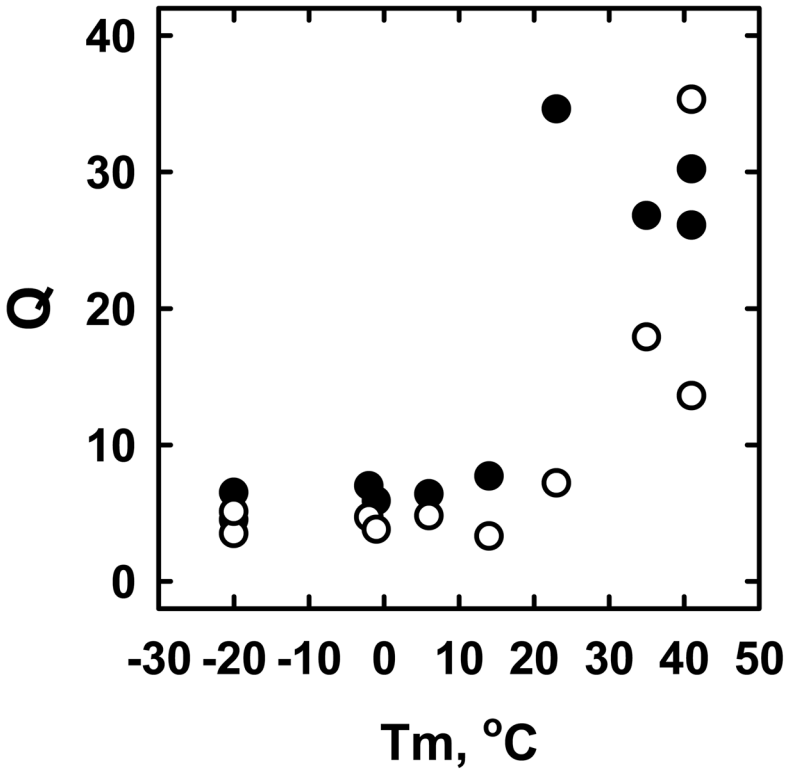

Figure 3.

Cholesterol distribution coefficients (Q) related to their thermal transition temperature, T_m. All of the cholesterol distribution coefficients (Q) were obtained using these mixtures: 10 mM MBCD, 0.8 mM LUV phospholipid and 0.1 mM cholesterol. Incubations were for 0.5 h at 25 °C (●) (n = 3–4) and 37 °C (○) (n = 2–3). T_m values were obtained from textbooks and, mostly, the Avanti Polar Lipids catalog. From left to right, the phospholipids are: DOPC, SOPS, POPC, DLPC, SOPC, POPS, DMPC, DMPS, DPPC and PSM. See the Q values in Table 1.

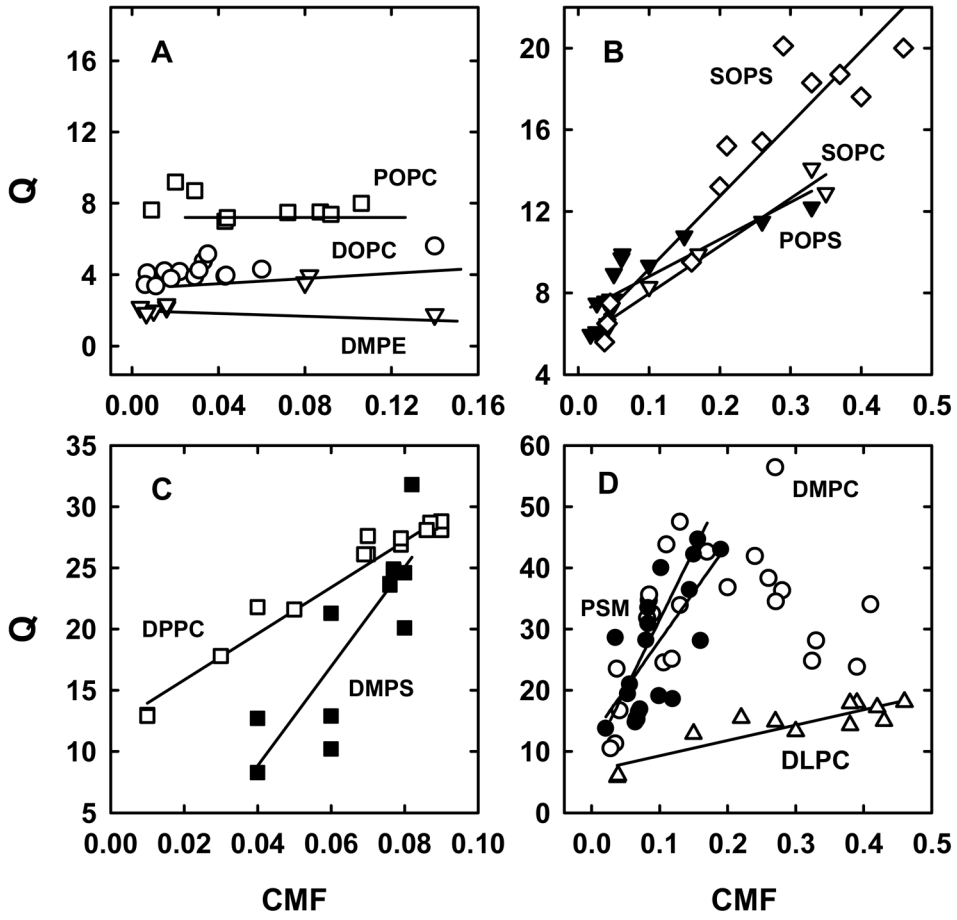

Figure 4.

Cholesterol distribution coefficients (Q) as a function of cholesterol mole fractions (CMF). Multiple experiments were performed for each curve by incubating 10 mM MBCD bearing 0.02 to 0.10 mM [^{14}C]cholesterol with 0.1–1.0 mM LUV phospholipid for 0.5 h at 25 °C. Solid lines are linear least squares fits. Panel A, POPC (□); DOPC (○); DMPE (▽). Panel B, SOPS (◇); SOPC (▽); POPS (▼). Panel C, DPPC (□); DMPS (■). Panel D, DLPC (△); PSM (●); DMPC, with a linear fit to the portion with a positive slope (○).

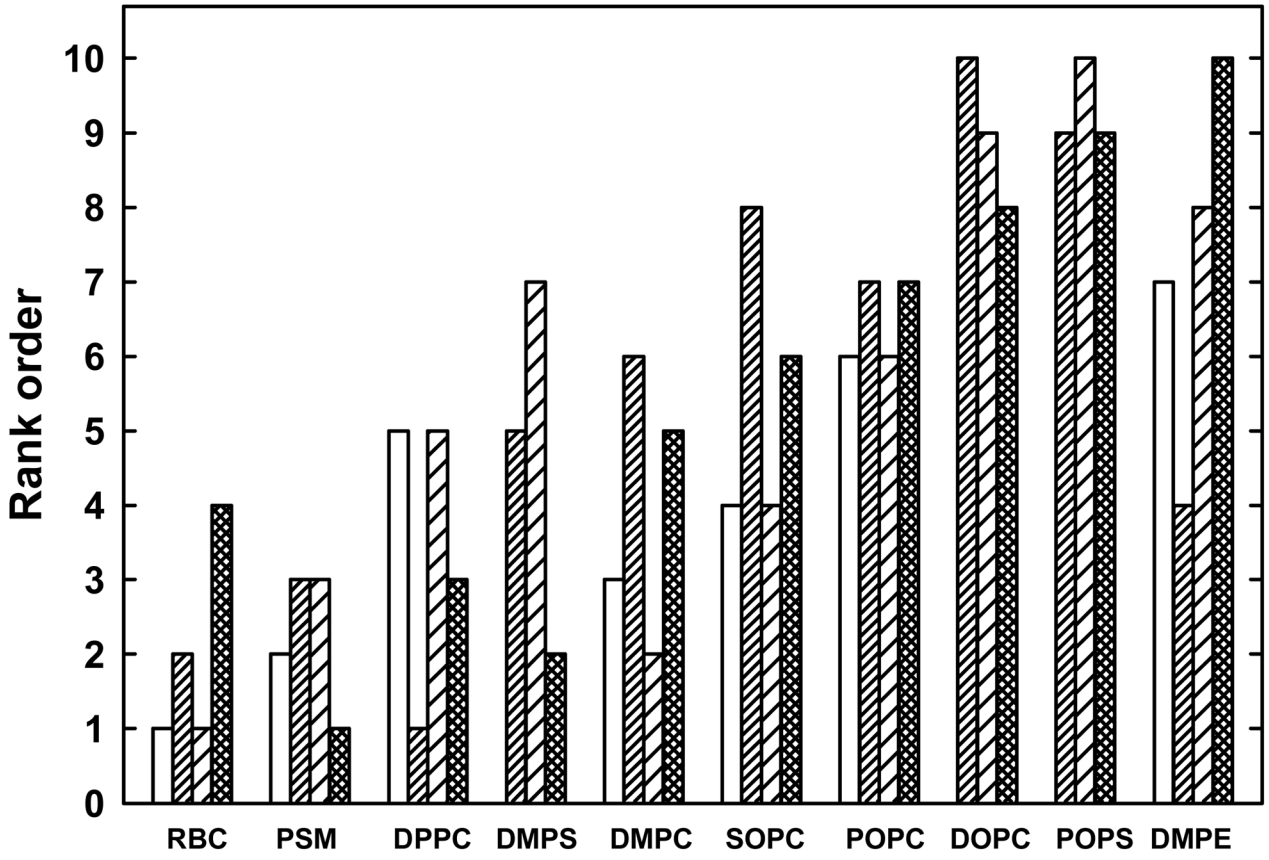

Figure 5.

Correlations of four measures of the strength of association between cholesterol and phospholipids. The four bars give the relative rankings from Table 1 for the respective values for the K_c, the RA of uncomplexed cholesterol, the % free cholesterol at the equivalence point, and Q. Rank 1 denotes the strongest association for a parameter. Values are not given for the K_c of the three phospholipids with stoichiometries of 1:2 and 2:3.

Table 1

Values for cholesterol-phospholipid complexes*

Lipid	Stoichiometry[a]	K_a[b]	RA of complexed cholesterol[c]	RA of uncomplexed cholesterol[d]	% uncomplexed cholesterol at the equivalence point[e]	Q[f]
PSM	1.2:1	4.2E3	0.47	15	2.0	35.3
DMPC	1:1	2.4E3	0.0026	50	1.9	7.2
SOPC	1:1	2.3E3	0.014	1600	2.6	4.8
DPPC	1:1	1.2E3	0.034	3	2.8	13.6
POPC	1:1	4.8E2	0.0024	1400	4.5	4.7
DMPE	1:1	1.3E2	0.011	20	8.5	2.3[g]
DMPS	2:3	5.9E5	0.011	35	6.3	17.9
DOPC	1:2	7.0E2	0.29	60000	10.7	3.5
POPS	1:2	1.6E2	7.4	1900	17.4	3.3
SOPS	no threshold detected					5.1
RBC	1:1	7.5E3	0.0030	13	1.0	10.5[h]

*Values in columns a-d were used to generate the curves in Figure 2; see Appendix 2.

[a]Cholesterol:phospholipid ratios (mol/mol).

[b]Association constants for cholesterol-phospholipid complexes; see eq. 8.

[c,d]Relative accessibilities of complexed and uncomplexed LUV cholesterol. Arbitrary units.

[e]% Uncomplexed cholesterol at the equivalence point, calculated using values in columns a–d.

[f]Cholesterol equilibrium distribution coefficient for mixtures containing 10 mM MBCD, 0.8 mM phospholipid and 0.1 mM cholesterol. T = 37 °C. n = 2–4. Exceptions: footnotes g and h.

[g]Assayed with 10 mM MBCD, 0.6 mM phospholipid P and 0.08 mM cholesterol at 25 °C.

[h]Assayed with 10 mM MBCD, 1–1.6 mM phospholipid P and 0.8–1.3 mM cholesterol at 37 °C.

n =3. The corresponding K_e value is 18.5; see eq. 2.